for the $\sigma$ and $\pi$ interactions with the ligand. The key difference between the two systems happens to be the electron count. In the $d^6$ "butterfly" $[Fe(PH_3)_4]^{2+}$ complex, the $\sigma$ orbital is occupied,[5b] while both $\sigma$ and $\pi$ orbitals are unoccupied in the $[ScCl_2]^+$ complex. This different occupation is reflected in the occupation or vacancy of one of the molecular orbitals of the transition state, namely an antibonding orbital between the metal and the extreme hydrogens. When this orbital is unoccupied ($[ScCl_2(H_3)]$) the metal is bound to these extreme hydrogens, thus leading to a four-membered ring. When this orbital is occupied ($[Fe(PH_3)_4(H_3)]^+$) the metal is bound only to the central hydrogen, thus leading to a "trefoil" topology.

## Conclusions

In this paper three different possible mechanisms for the intramolecular exchange of a hydrogen atom between the hydride and molecular hydrogen ligands in octahedral $d^6$ *cis*-$[Fe(PR_3)_4H(H_2)]^+$ complexes have been considered. One of them happens to be by far the most favored, with an energetic barrier of only 3.2 kcal/mol. This mechanism is the so-called open direct transfer mechanism and consists essentially of a single step transfer of the hydrogen atom between the two ligands, while the three hydrogen atoms are in a linear-like arrangement. The low barrier of ca. 3 kcal/mol agrees with the experimental observation of an easy exchange between the molecular hydrogen and hydride ligands. Moreover, the barrier is so small that this mechanism can even be claimed to be operative for the trans octahedral structures, via a small amount of the cis isomer in equilibrium with the trans isomer. Actually, the efficiency of this mechanism demonstrated here rejoins the few evidences supporting an active role of molecular hydrogen complexes in the breaking of the strong H-H bond.

Besides the importance of the very molecular hydrogen complexes, it is also interesting to set the results of this paper into the framework of current ideas on $\sigma$-bond activation by transition-metal complexes. The two main mechanisms proposed so far are (a) oxidative addition, acting on electron-rich systems, with late transition metals, and (b) $\sigma$-bond metathesis (also called heterolytic activation), acting on electron-poor systems, typically early transition metal or rare-earth complexes. The mechanism reported here seems to lie outside this scheme. It takes place with a relatively electron-rich $d^6$ complex of iron and has formal resemblances to heterolytic activation. Furthermore, the electron topology in the transition state shows it is absolutely different from traditional $\sigma$-bond metathesis. Thus, it could be envisioned as the first characterized example of a new kind of activation mechanism for $\sigma$ bonds. Actually, this mechanism could also be acting in some reactions that have been considered so far to be oxidative additions.

Although generalization of the results presented here might be questioned by the limitations of the applied methodology, we think that the interest of this subject and the important implications suggested by these results make its presentation and prosecution of research in this area definitely worthy.

**Acknowledgment.** This work received financial support from the Spanish "Dirección General de Investigación Científica y Técnica" under Project No. PB86-0529. Partial support has also been received from the Universitat Autònoma de Barcelona through the Program for Precompetitive Research Groups, 1991.

---

# Transition Metal Polyhydride Complexes. 2. Theoretical Methods for the Determination of Stabilities of Classical and Nonclassical Isomers

**Zhenyang Lin and Michael B. Hall***

*Contribution from the Department of Chemistry, Texas A&M University, College Station, Texas 77843.*
*Received September 19, 1991*

**Abstract:** Ab initio calculations with effective core potentials have been used to study the relative stability of classical and nonclassical isomers of the model complexes, $IrH_5L_2$ (L = Be, $PH_3$, and $PMe_3$). The examination of different levels and techniques of electron correlation suggests that the second-order Moller-Plesset (MP2) method will provide a reliable prediction of the stability of one isomer over the other. The conventional substitution of a $PR_3$ ligand by $PH_3$ in quantum chemical calculations has also been examined. The small error (ca. 2 kcal/mol) caused by this replacement suggests that it is a reasonable choice in this class of transition metal polyhydride complexes. Our results on the electronic structural difference between classical and nonclassical isomers suggest that the nonclassical isomer is preferred for complexes with strong $\pi$ acceptor ligands and contracted central-metal d orbitals.

## Introduction

Since the first discovery of a stable nonclassical dihydrogen complex, $W(CO)_3[P(i\text{-}Pr)_3]_2(\eta^2\text{-}H_2)$, by Kubas et al.,[1] transition metal polyhydride complexes have been the subject of considerable interest.[2-25] The intensive studies in this subject have resulted in the discovery of many complexes containing nonclassical or classical isomers in solution. However, only a few $\eta^2$-$H_2$ complexes

---

[1] (a) Kubas, G. J.; Ryan, R. R.; Swanson, B. J.; Vergamini, P. J.; Wasserman, H. J. *J. Am. Chem. Soc.* **1984**, *106*, 451. (b) Kubas, G. J.; Ryan, R. R.; Wroblewski, D. *J. Am. Chem. Soc.* **1986**, *108*, 1339. (c) Kubas, G. J.; Unkefer, C. J.; Swanson, B. J.; Fukushima, E. *J. Am. Chem. Soc.* **1986**, *108*, 7000. (d) Kubas, G. J. *Acc. Chem. Res.* **1988**, *21*, 120.

[2] (a) Sweany, R. L. *J. Am. Chem. Soc.* **1985**, *107*, 2374. (b) Upmacis, R. K.; Poliakoff, M.; Turner, J. *J. Am. Chem. Soc.* **1986**, *108*, 3645.

[3] (a) Bautista, M. T.; Earl, K. A.; Morris, R. H.; Sella, A. *J. Am. Chem. Soc.* **1987**, *109*, 3780. (b) Bautista, M. T.; Earl, K. A.; Maltby, P. A.; Morris, R. H.; Schweitzer, C. T.; Sella, A. *J. Am. Chem. Soc.* **1987**, *109*, 3780. (c) Earl, K. A.; Polito, M. A.; Morris, R. H. *J. Am. Chem. Soc.* **1987**, *109*, 3780.

[4] (a) Morris, R. H.; Sawyer, J. F.; Shiralian, M.; Zubkowski, J. D. *J. Am. Chem. Soc.* **1985**, *107*, 5581. (b) Ricci, J. S.; Koetzle, T. F.; Bautista, M. T.; Hofstede, T. M.; Morris, R. H.; Sawyer, J. F. *J. Am. Chem. Soc.* **1989**, *111*, 8823.

0002-7863/92/1514-2928$03.00/0

have been unequivocally characterized in the solid state by both X-ray and neutron diffraction techniques,[1,4] while the existence of most other $\eta^2$-$H_2$ complexes has been inferred mainly by NMR spectroscopic studies or X-ray crystallographic determinations without locating the positions of hydrogens. In the spectroscopic studies, the $^1H$ NMR relaxation time ($T_1$) has been used as a criterion to discern classical and nonclassical structures in solutions. Recent studies[11,12] have revealed that several examples of polyhydrides, originally identified as having nonclassical structures according to this criterion, e.g., $ReH_7$(dppe) (dppe = 1,2-bis(diphenylphosphino)ethane) and $ReH_5(PPh_3)_3$, are classical polyhydrides. The absolute validity of this criterion is, therefore, called into question.[19]

All these exciting experimental results led to an increasing number of quantum chemical studies of their electronic structures and the relative energies of classical and nonclassical isomers.[21-25] Most of these studies have been restricted to semiempirical calculations or to ab initio calculations at the Hartree–Fock (HF) level. Examination of electron correlation suggested that it is extremely important in determining the relative stability of classical and nonclassical isomers.[25b,26] For example, in the calculations of $ReH_7(PH_3)_2$ polyhydride complexes, HF gave a stable nonclassical isomer while CI gave a stable classical one.[26] In this paper, we will examine the use of different levels of electron-correlation calculations on model complexes, $IrH_5L_2$ (L = Be, $PH_3$, and $PMe_3$), to determine their reliability. This study will allow us to examine the accuracy of given methods and, therefore, to choose a reliably rapid one to determine the structure of these hydrides.

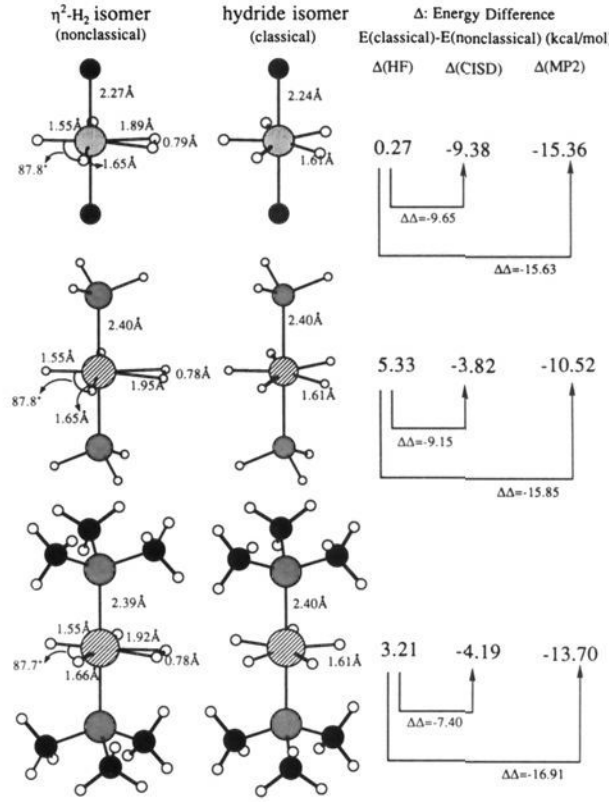

**Figure 1**. Geometries of HF optimized model complexes, $IrH_5L_2$ (L = Be, $PH_3$, and $PMe_3$) and their total energy differences at HF, CISD, and MP2 levels.

## Theoretical Details

In the model complexes, $IrH_5L_2$ (L = Be, $PH_3$, and $PMe_3$), the Ir–P–H, Ir–P–C, and P–C–H angles were fixed to be 115°, 110.1° (from experimental value of $Ir(H)_5[P(i\text{-}Pr)_3]_2$),[15] and 109.47°, respectively. The P–C, P–H, and C–H bond distances were also fixed by using standard bond lengths.[27] The remaining geometric parameters were optimized at the restricted Hartree–Fock (HF) level.

*In the effective core potentials (ECPs), for Ir atom,*[28] *the [Kr]4d$^{10}$ core* was replaced by the ECP, and the remaining electrons, corresponding to the $5s^25p^65d^86s^1$ configuration, were treated explicitly in the calculations. The largest basis set, (541/41/111), corresponds to a double-$\zeta$ representation of the 6s/5p electrons and a triple-$\zeta$ representation of the 5d electrons. For ligand atoms, the ECPs and basis sets (double-$\zeta$ for P atom and single-$\zeta$ for C atom) of Stevens, Basch, and Krauss were used.[29] [He] and [Ne] configurations were taken as cores for the C and P atoms. The Dunning–Huzinaga's double-$\zeta$ basis set (31)[30] was used for H atoms of $PH_3$ ligands and those directly bonded to the central metal atom, while the corresponding contracted basis (4) was used for H atoms of $P(Me)_3$ ligands. For Be atom, an unsplit (33) basis set was used.[31,32]

To study the effect of basis sets, we used both a smaller and a larger basis set for both Ir and H atoms on the Be model. In the smaller basis set, (541/41/21), we contracted the Ir basis set derived from ECP above. In the larger one, (541/41/111) for Ir and (31/1) for H atoms, we augmented the H atom with polarized functions ($\zeta_p \approx 1.0$).

The configuration interaction calculations with all-single-and-double excitations (CISD) used the HF results as starting solutions and the

---

(5) Albertin, G.; Antoniatti, S.; Bordignon, E. *J. Am. Chem. Soc.* **1989**, *111*, 2072.

(6) (a) Chinn, M. S.; Heinekey, D. M.; Payne, N. G.; Sofield, C. D. *Organometallics* **1989**, *8*, 1824. (b) Chinn, M. S.; Heiekey, D. M. *J. Am. Chem. Soc.* **1987**, *109*, 5865.

(7) Hart, D. W.; Bau, R.; Koetzle, T. F. *J. Am. Chem. Soc.* **1977**, *99*, 7557.

(8) Howard, J. A. K.; Johnson, O.; Koetzle, T. F.; Spencer, J. L. *Inorg. Chem.* **1987**, *26*, 2930.

(9) Lyons, D.; Wilkinson, G.; Thornton-Pett, M.; Hursthouse, M. B. *J. Chem. Soc., Dalton Trans.* **1984**, 695.

(10) Gregson, D.; Mason, S. A.; Howard, J. A. K.; Spencer, J. L.; Turner, D. G. *Inorg. Chem.* **1984**, *23*, 4103.

(11) (a) Cotton, F. A.; Luck, R. L. *Inorg. Chem.* **1989**, *28*, 2181. (b) Cotton, F. A.; Luck, R. L. *J. Am. Chem. Soc.* **1989**, *111*, 5757. (c) Cotton, F. A.; Luck, R. L. *J. Chem. Soc., Chem. Commun.* **1988**, 1277.

(12) (a) Howard, J. A. K.; Mason, S. A.; Johnson, O.; Diamond, I. C.; Crennell, S.; Keller, P. A. *J. Chem. Soc., Chem. Commun.* **1988**, 1502. (b) Brammer, L.; Howard, J. A. K.; Johnson, O.; Koetzle, T. F.; Spencer, J. L.; Stinger, A. M. *J. Chem. Soc., Chem. Commun.* **1991**, 241.

(13) (a) Luo, X. L.; Baudry, D.; Boydell, P.; Charpin, P.; Nierlich, M.; Ephritikhine, M.; Crabtree, R. H. *Inorg. Chem.* **1990**, *29*, 1511. (b) Luo, X. L.; Schutle, G. K.; Demoll, P.; Crabtree, R. H. *Inorg. Chem.* **1990**, *29*, 4268.

(14) Luo, X. L.; Crabtree, R. H. *J. Am. Chem. Soc.* **1990**, *112*, 6912.

(15) Garlaschelli, L.; Khan, S. I.; Bau, R.; Longoni, G.; Koetzle, T. F. *J. Am. Chem. Soc.* **1985**, *107*, 7212.

(16) (a) Hamilton, D. G.; Crabtree, R. H. *J. Am. Chem. Soc.* **1988**, *110*, 4126. (b) Crabtree, R. H.; Lavin, M.; Bonneviot, L. *J. Am. Chem. Soc.* **1986**, *108*, 4032.

(17) Mediati, M.; Tachibana, G. N.; Jensen, C. M. *Inorg. Chem.* **1990**, *29*, 5.

(18) (a) Lundquist, E. G.; Huffman, J. C.; Folting, K.; Caulton, K. G. *Angew. Chem., Int. Ed. Engl.* **1988**, *27*, 1165. (b) Lundquist, E. G.; Folting, K.; Streib, W. E.; Huffman, J. C.; Eisenstein, O.; Caulton, K. G. *J. Am. Chem. Soc.* **1990**, *112*, 855.

(19) Desrosiers, P. J.; Cai, L.; Lin, Z. R.; Richards, R.; Halpern, J. *J. Am. Chem. Soc.* **1991**, *113*, 4173.

(20) (a) Heinekey, D. M.; Millar, J. M.; Koetzle, T. F.; Payne, N. G.; Zilm, K. W. *J. Am. Chem. Soc.* **1990**, *112*, 909. (b) Zilm, K. W.; Heinekey, D. M.; Millar, J. M.; Payne, G. N.; Neshyba, S. P.; Duchamp, J. C.; Szczyrba, J. *J. Am. Chem. Soc.* **1990**, *112*, 920.

(21) (a) Hay, P. J. *J. Am. Chem. Soc.* **1987**, *109*, 705. (b) Eckart, J.; Kubas, G. J.; Hall, J. H.; Hay, P. J.; Boyle, C. M. *J. Am. Chem. Soc.* **1990**, *112*, 2324.

(22) (a) Burdett, J. K.; Mohammad, R. P. *Organometallics* **1987**, *6*, 1684. (b) Burdett, J. K.; Phillips, J. R.; Mohammad, R. P. *Inorg. Chem.* **1987**, *26*, 3054.

(23) Pacchioni, G. *J. Am. Chem. Soc.* **1990**, *112*, 80.

(24) Maseras, F.; Duran, M.; Lledos, A.; Bertran, J. *J. Am. Chem. Soc.* **1991**, *113*, 2879.

(25) (a) Part 1: Lin, Z.; Hall, M. B. *Inorg. Chem.* **1991**, *30*, 2569. (b) Part 3: Lin, Z.; Hall, M. B. *J. Am. Chem. Soc.* **1992**, *114*, in press.

(26) Haynes, G. R.; Martin, R. L.; Hay, P. J. *J. Am. Chem. Soc.* **1992**, *114*, 28.

(27) Hehre, W. J.; Ditchfield, R.; Stewart, R. F.; Pople, J. A. *J. Chem. Phys.* **1970**, *52*, 2769.

(28) Hay, P. J.; Wadt, W. R. *J. Chem. Phys.* **1985**, *82*, 299.

(29) Stevens, W. J.; Basch, H.; Krauss, M. *J. Chem. Phys.* **1984**, *81*, 6026.

(30) (a) Huzinaga, S. *J. Chem. Phys.* **1965**, *42*, 1293. (b) Dunning, T. H., Jr. *J. Chem. Phys.* **1970**, *53*, 2823.

(31) *Gaussian Basis Sets for Molecular Calculations*; Huzinaga, S., Ed.; Elsevier: Amsterdam, 1984.

(32) Simpson, C. Q.; Hall, M. B.; Guest, M. F. *J. Am. Chem. Soc.* **1991**, *113*, 2898.

ground states as the single reference. The active space of the CISD calculations includes all the valence orbitals. In the intermediate basis set, complete-active-space self-consistent-field calculations[33] (CASSCF) were performed on the $Ir(H)_5Be_2$ and $Ir(H)_3Be_2(\eta^2\text{-}H_2)$ isomers with an active space of the five occupied valence orbitals and the corresponding five virtual ones in the (Ir–H's) equatorial plane. Two multireference configuration-interaction (MRCI) calculations were made based on the solutions of CASSCF calculations. MRCI(1) contains all single and double excitations from all reference configurations in the CASSCF with coefficients greater than 0.045 (thresholds of 0.10 and 0.05 were used in MRCI calculations by other authors)[34] within all orbital space. The hydride isomer has 12 such configurations while the $\eta^2\text{-}H_2$ isomer has 7. MRCI(2) takes 12 configurations for each isomer with greatest coefficients in CASSCF as reference configurations. The second-order Moller–Plesset (MP2) perturbation calculations[35] were carried out for all model complexes. The MP3 and MP4 (with single, double, triple, and quadruple substitutions) calculations were also performed on Be model isomers.

All HF, CISD, CASSCF, and MRCI calculations were performed with the GAMESS package,[36] while all MP calculations were made by the use of Gaussian 88 program.[37] The Laplacian of valence electron density was plotted with the use of the program MOPLOT.[38] All GAMESS calculations were made at the Cornell National Supercomputer Facility (CNSF) on an IBM 3090-600VF, at the Supercomputer Center of Texas A&M University on a Cray Y-MP2/116, or at the Chemistry Department on a FPS Model 522. Gaussian 88 was run at CNSF.

## Results and Discussion

**Hartree–Fock, CISD, and MP2 Calculations.** Initially, we optimized the model complexes, $IrH_5L_2$ (L = Be, $PH_3$, and $PMe_3$), with the intermediate basis set at the HF level with five hydrogen atoms occupying the equatorial plane of a pentagonal bipyramid and two L ligands on the axial positions. The two phosphine ligands were staggered according to the crystal structure of $IrH_5[P(i\text{-}Pr)_3]_2$.[15] The overall symmetry is $C_s$ with a mirror passing through the two L's, Ir, and one of the five H atoms. For each model complex, two local HF minima[39] were found, which correspond to a classical and a nonclassical hydride isomer. The results are shown in Figure 1. As we can see, at the HF level the $\eta^2\text{-}H_2$ isomer is always more stable than the classical one although for L = Be the isomers are almost of equal energy. However, the single-crystal X-ray and neutron diffraction analysis of $IrH_5[P(i\text{-}Pr)_3]_2$[15] indicated that the $IrH_5P_2$ core is a pentagonal bipyramidal geometry with the 5 H atoms occupying the equatorial plane, a classical iridium polyhydride complex. Apparently, HF calculations overestimate the stability of nonclassical isomers.

It is clear that the experimental result may be reproduced if we include electron correlations. First, we did CISD and MP2 calculations for all three models (two isomers for each model) based on the HF optimized structures. Results are also shown in Figure 1. Both CISD and MP2 results predict the classical isomers as stable isomers. The importance of electron correlation (EC) is obvious from these calculations. The significant difference between the two methods of electron-correlation calculations should also be noted. In the figure, $\Delta E$ was defined as the energy difference between two isomers:

$$\Delta E = E(\text{classical isomer}) - E(\text{nonclassical isomer})$$

We also defined correlation energy difference as

$$\Delta\Delta E = [E(\text{EC}) - E(\text{HF})]_{\text{classical isomer}} - [E(\text{EC}) - E(\text{HF})]_{\text{nonclassical isomer}} = \Delta E(\text{EC}) - \Delta E(\text{HF})$$

where EC is either CISD or MP2. It can be seen from Figure 1 that $\Delta\Delta E$'s for all three model are close to each other (the biggest difference is 2.25 kcal/mol for CISD calculations and 1.28 kcal/mol for MP2). This indicates that the correlation energy difference is mainly due to the difference in Ir–H and H–H interactions in the equatorial plane of the two isomers. This result conveniently allows us to select the Be model with the intermediate basis set to study higher levels of electron correlation and keep the computational expense reasonable. In a previous paper,[32] it has been shown that calculations on model complexes with substitution of $PR_3$ groups by Be's successfully predicted the unexpected difference in the ground states of $Ti(CH_3)_2(dppe)_2$ and $TiCl_2(dppe)_2$ complexes. In the $IrH_5Be_2$ model, we could adjust the Ir–Be distance (ca. 2.50 Å) to obtain a $\Delta E$(HF) equal to the $\Delta E$(HF) of $IrH_5(PMe_3)_2$ model so that Be faithfully mimics the $PMe_3$ ligand. However, the purpose of the use of the Be model in this work is to examine the accuracy of different levels of electron correlation calculations in calculating the energy difference, which is mainly due to the difference in the Ir–H and H–H interactions, between classical and nonclassical isomers. Therefore, we used the optimized structures discussed above for further studies.

**Higher Levels of Electron Correlation.** With the Be model, $IrH_5Be_2$, the HF results for both isomers (see Figure 1) were used as starting solutions to perform 10-electron, 10-orbital CASSCF, which includes the five occupied valence orbitals and five corresponding virtual orbitals in the Ir–H equatorial plane. The five occupied orbitals are, in fact, the five Ir–H bonding orbitals for the classical isomer and the three Ir–H bonding orbitals, one H–H bonding orbital and one 5d nonbonding orbital for the nonclassical isomer. Then, the CASSCF results were used for the multireference configuration interaction (MRCI) calculations. The details of the MRCI calculations have been described in the Theoretical Details section. The MRCI(1) calculations gave an energy difference ($\Delta E$) of −15.77 kcal/mol between the two isomers with 697 599 and 285 266 configurations for the classical and nonclassical isomers, respectively, while the MRCI(2) results gave an energy difference of −14.02 kcal/mol with 697 599 and 685 430 configurations, respectively. In these MRCI calculations, the reference configurations chosen from the CASSCF results continued to dominate in the resulting wave functions. Therefore, an energy difference of ca. −15 kcal/mol can be predicted from our MRCI calculations. MP2 calculations gave an energy difference of −15.36 kcal/mol between the classical and nonclassical isomers for Be model while CISD gave only −9.38 kcal/mol. In addition, we also did MP3 and MP4 calculations on the Be model. All these results are listed in Table I. The CISD calculation severely underestimates the energy difference, while the more accurate MP4 result is very close to MRCI results; neither differs much from MP2 result. Thus, MP2 calculations are a reasonable choice for determining the relative stability of classical and nonclassical hydride complexes, especially given the computational expense of the more accurate MP4 and MRCI calculations.

**Models and Basis Sets.** We examine the effect of the widely used substitution of $PR_3$ by $PH_3$ in quantum chemical calculations through a comparison of $PMe_3$ and $PH_3$. The results show that HF optimized structures of $PMe_3$ model are very similar to those of $PH_3$ model (see Figure 1). The HF calculations gave an energy difference between the two isomer of 5.33 kcal/mol for the $PH_3$ model and 3.21 kcal/mol for the $PMe_3$ model, while the MP2 calculations gave a difference of −10.52 kcal/mol for the $PH_3$ model and −13.70 kcal/mol for the $PMe_3$ model. Thus, the $PH_3$ substitution slightly overestimates the stability of the nonclassical isomer. This result arises from the $PH_3$ ligands' weaker $\sigma$ donor

---

(33) (a) Jonesson, B.; Roos, B. O.; Taylor, P. R.; Siegbahn, P. E. M. *J. Chem. Phys.* **1981**, *74*, 4566. (b) Roos, B. O.; Linse, P.; Siegbahn, P. E. M.; Bloomburg, M. P. A. *Chem. Phys.* **1976**, *66*, 197. (c) Knowles, P. J.; Sexton, G. J.; Handy, N. C. *Chem. Phys.* **1982**, *72*, 337.

(34) (a) Lindberg, P.; Noreus, D.; Blomberg, M. R. A.; Siegbahn, P. E. M. *J. Chem. Phys.* **1986**, *85*, 4530. (b) Petterson, L. G. M.; Siegbahn, P. E. M. *J. Chem. Phys.* **1985**, *83*, 3538.

(35) (a) Moller, C.; Plesset, M. S. *Phys. Rev.* **1936**, *46*, 618. (b) Pople, J. A.; Binkley, J. S.; Seeger, R. *Int. J. Quantum Chem.* **1976**, *S10*, 1.

(36) Guest, M. F. Daresbury Laboratory, Warrington, WA4 4AD, U.K.

(37) Frisch, M. J.; Head-Gordon, M.; Schlegel, H. B.; Raghavachari, K.; Binkley, J. S.; Gonzalez, C.; Defrees, D. J.; Fox, D. J.; Whiteside, R. A.; Seeger, R.; Melius, C. F.; Baker, J.; Martin, R. L.; Kahn, L. R.; Stewart, J. J. P.; Fluder, E. M.; Topiol, S.; Pople, J. A. *Gaussian 88*; Gaussian, Inc.: Pittsburgh, PA.

(38) Interactive MOPLOT: a package for the interactive display and analysis of molecular wave functions incorporating the programs MOPLOT (D. Lichtenburger), PLOTDEN (R. F. W. Bader, D. J. Kenworthy, P. M. Beddal, G. R. Runtz, and S. G. Anderson), SCHUSS (R. F. W. Bader, G. R. Runtz, S. G. Anderson, and F. W. Biegler–Koenig), and EXTREM (R. F. W. Bader and F. W. Biegler–Koenig): P. Sherwood and P. J. MacDougall, 1989.

(39) When geometry optimization is converged, we view the resulting point as a local minimum.

**Table I.** Total Energy and Energy Difference between Two Isomers of the $IrH_5(Be)_2$ Model at Different Levels of Theory

| basis set | | | | | |
|---|---|---|---|---|---|
| Ir basis | H basis | calcn[a] | $IrBe_2H_3(\eta\text{-}H_2)$ (au) | $IrBe_2H_5$ (au) | energy diff Δ (kcal/mol) |
| (541/41/21) | (31) | HF | −135.5391 | −135.5381 | 0.58 |
| | | CISD | −135.7169 | −135.7322 | −9.55 |
| | | MP2 | −135.7520 | −135.7755 | −14.72 |
| | | MP3 | −135.7425 | −135.7632 | −12.97 |
| | | MP4 | −135.7733 | −135.7956 | −14.01 |
| (541/41/111) | (31) | HF | −135.5421 | −135.5416 | 0.27 |
| | | CISD | −135.7338 | −135.7495 | −9.38 |
| | | CASSCF | −135.6285 | −135.6459 | −10.93 |
| | | MRCI(1) | −135.7863 | −135.8114 | −15.77 |
| | | MRCI(2) | −135.7891 | −135.8114 | −14.02 |
| | | MP2 | −135.7966 | −135.8211 | −15.36 |
| | | MP3 | −135.7848 | −135.8068 | −13.79 |
| | | MP4 | −135.8198 | −135.8436 | −14.96 |
| (541/41/111) | (31/1) | HF | −135.5646 | −135.5650 | −0.29 |
| | | CISD | −135.7926 | −135.8105 | −11.24 |
| | | MP2 | −135.8674 | −135.8987 | −19.66 |
| | | MP3 | −135.8536 | −135.8800 | −16.52 |
| | | MP4 | −135.8919 | −135.9207 | −18.10 |

[a] CISD: including all the valence orbitals in the active space. CASSCF: having the active space of the five occupied valence orbitals and the five corresponding virtual ones in the equatorial plane. MRCI(1): containing all single and double excitations from all reference configurations in the CASSCF with coefficients greater than 0.045 within all orbital space. The hydride isomer has 12 configurations while the hydrogen isomer has 7. MRCI(2): 12 configurations for each isomer with larger coefficients in CASSCF are taken as reference configurations.

property. A stronger σ donor, such as $PMe_3$, pushes electron density onto the central metal atom, making it more easily oxidized and favoring the dihydride over dihydrogen isomer. Thus, a $PH_3$ model always overestimates the stability of the nonclassical isomer; i.e., if the $PH_3$ model predicts a classical hydride isomer as most stable it is correct, while if it predicts a nonclassical isomer as most stable the accuracy of the prediction depends on the magnitude of the energy difference and the type of $PR_3$ ligands. The σ donating abilities of $PR_3$ (the three R groups can be H, aryl, and alkyl or mixture of them) ligands in most hydride complexes are between the poor σ donor $PH_3$ and the strong σ donor $PMe_3$. Therefore, the $PH_3$ model is still a reasonable choice for most calculations.

For the completeness of this study, we used the Be model, $IrBe_2H_5$, to examine the effect of basis sets. Two additional types of basis sets described in the Theoretical Details were used to optimize the model complex, $IrBe_2H_5$, at the HF level. Again, two local minima,[39] which correspond to a classical and a nonclassical isomer, were found for both basis sets. The optimized structures from different basis sets are almost identical. Electron correlation calculations with CISD, MP2, MP3, and MP4 were also performed based on the HF optimized structures. All these results are also listed in Table I. It can be seen from the table that all HF results predict both classical and nonclassical isomers of almost equal energies, while all electron correlation calculations give a stable classical isomer at least 10 kcal/mol lower in energy. Although the classical isomer gains 2 to 3 kcal/mol correlation energy from the intermediate basis set to the largest one (the addition of polarization function on H), we see that electron correlation itself is far more important than the basis set in determining the stability of classical and nonclassical isomers. Thus, the use of the intermediate basis set will be essentially enough to provide qualitatively correct results.

**Electronic Structural Analysis.** The factors that stabilize one isomer over the other will be discussed in detail for a variety of complexes in a subsequent paper. Here, we provide a glimpse of the electronic structural difference between the two isomers. The plots of the Laplacian of the valence electron density, i.e., $\nabla^2\rho$,[40] from the ab initio HF results of the two $PMe_3$ model isomers in the equatorial plane (i.e., Ir–H plane) are shown in Figure 2.[41]

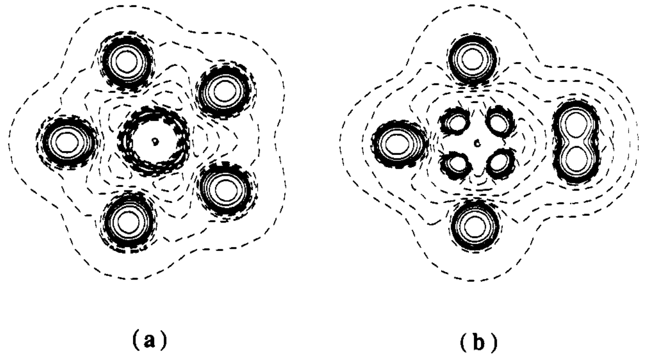
(a) (b)

**Figure 2.** Plots of $-\nabla^2\rho$ on the equatorial plane of $PMe_3$ model complex, $IrH_5(PMe_3)_2$: (a) hydride isomer and (b) $\eta^2$-$H_2$ isomer.

**Scheme I**

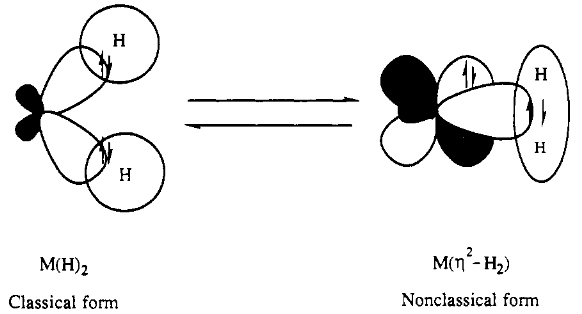

In the contour plots, solid lines denote $-\nabla^2\rho > 0$, where the electron charge is locally concentrated, and dashed lines denote $-\nabla^2\rho < 0$, where the electron charge is locally depleted. For the hydride isomer, Figure 2a, the electron charges are concentrated mainly on the H atoms. Five small concentrations are observed in the valence region of the central Ir atom, which are located in the Ir–H bond directions, and indicate covalent bond character between Ir and H. For the $\eta^2$-$H_2$ isomer, in Figure 2b, three H atoms are bonded to the Ir through the depletions around the central atom, as is usual for dative bonds. Four concentrations appear around the central Ir atom, which are contributions from the occupied valence 5d orbital in the equatorial plane. It also can be seen that the $\eta^2$-$H_2$ ligand is weakly bonded to the central metal atom. Based on the analysis of the Laplacian of the valence electron density on the $PMe_3$ model isomers, an illustrative bonding scheme (see Scheme I) is proposed to describe the difference of between classical and nonclassical forms. In the classical form,

---

(40) (a) Bader, R. F. W.; MacDougall, P. J.; Lau, C. D. H. *J. Am. Chem. Soc.* **1984**, *106*, 1594. (b) Bader, R. F. W. *Acc. Chem. Res.* **1985**, *18*, 9.

(41) The plots of the Laplacian of the valence electron density from both HF and MRCI results of Be model isomers in the Ir–H plane show that the properties of the valence electron density calculated from HF and MRCI wave functions are qualitatively equivalent. Therefore, the HF results were used to do the Laplacian calculations on $PMe_3$ model isomers.

the central metal atom donates its d electrons to H atoms and forms metal–hydrogen bonds. In the nonclassical isomer, the central metal atom retains its d electrons in the d nonbonding orbital. Therefore, the stability of the $\eta^2$-$H_2$ isomer largely depends on the strength of d-electron transfer to H. It can be deduced that for a complex with strong $\pi$ acceptor ligands and contracted central metal d orbitals, a nonclassical isomer is possibly preferred.

## Summary

Examination of different electron correlation techniques for calculating the relative energies of classical and nonclassical hydride isomers suggests that the MP2 method provides a reliable result. The CISD method underestimates the stability of the classical hydride isomer. The effect of basis sets is relatively small when compared with the effect of electron correlation. Therefore, a moderate sized basis set can provide a qualitatively correct result. The conventional substitution of $PR_3$ ligands by $PH_3$ in quantum chemical calculations has also been examined for the investigated isomers. In general, $PH_3$ replacement is a reasonable procedure in this class of transition metal complexes. The electronic structural difference between classical and nonclassical isomers suggest that the nonclassical isomer is preferred for complexes with strong $\pi$ acceptor ligands and contracted central metal d orbitals.

**Acknowledgment.** We thank the National Science Foundation (Grant No. CHE 91-13634) and the Robert A. Welch Foundation (Grant No. A-648) for financial support and M. F. Guest for providing the GAMESS package of programs. This research was conducted in part with use of the Cornell National Supercomputer Facility, a resource for the Center for Theory and Simulation in Science and Engineering at Cornell University, which is funded in part by the National Science Foundation, New York State, and the IBM Corp.

---

# Lacunary Polyoxometalate Anions Are $\pi$-Acceptor Ligands. Characterization of Some Tungstoruthenate(II,III,IV,V) Heteropolyanions and Their Atom-Transfer Reactivity

**Chaoying Rong and Michael T. Pope***

*Contribution from the Department of Chemistry, Georgetown University, Washington, D.C. 20057.*

*Received July 19, 1991*

**Abstract:** Reaction of $[Ru(H_2O)_6]^{2+}$ with $[PW_{11}O_{39}]^{7-}$, followed by oxidation with $O_2$ yields $[PW_{11}O_{39}Ru^{III}(H_2O)]^{4-}$ (**1**) isolated as the cesium salt. Cyclic voltammetry shows that **1** is reducible/oxidizable to the corresponding aquaruthenium(II) (**2**), oxoruthenium(IV), and oxoruthenium(V) derivatives. The p$K_a$ of **1** is 5.1, determined from a ca. 300 ppm shift of the $^{31}P$ NMR line between pH 3 and 6. At pH 3.0 and 23 °C the rate of electron transfer between **1** and **2** was determined by $^{31}P$ NMR line-broadening to be $1.2 \times 10^6$ $M^{-1}$ $s^{-1}$. **2** reacts with pyridine, sulfoxides, dialkyl sulfides, and active alkenes (maleic, fumaric, crotonic acids, 1,4-dihydroxybut-2-ene) to form $[PW_{11}O_{39}Ru^{II}(L)]^{5-}$ species, which are oxidizable to the $Ru^{III}$ stage only. At pH 3.0 and 20 ± 1 °C the half-life for substitution of DMSO for water on **2** is 3.5 h ($k_{obs} = 5.5 \times 10^{-5}$ $s^{-1}$) and this rate is some 3 orders of magnitude slower than that for water exchange on $[Ru(H_2O)_6]^{2+}$. The electronic spectra of the $Ru^{II}$ derivatives show, in addition to the expected d–d bands, broad intense charge-transfer absorption attributed to $Ru^{II} \rightarrow W^{VI}$. Tungsten-183 NMR spectra of **2** and the dimethyl sulfoxide and maleic acid derivatives show the expected six-line (2:2:2:1:2:2) pattern but with resonances for the W atoms adjacent to Ru deshielded by as much as ca. 360 ppm. This effect is greatest for **2** ($L = H_2O$) and least for L = maleic acid and is attributed to a partial delocalization of Ru $\pi$-electron density onto the polytungstate ligand. The anomalous redox potential for $Ru^{III/II}$ in **2** (in comparison to other $M^{III/II}$ couples in $[PW_{11}O_{39}M(H_2O)]^{5-}$) is a further indicator of electron delocalization. In acidic solution, pH ~ 0, **1** is oxidized to the oxoruthenium(V) derivative in a single two-electron step, and this forms the basis of an electrocatalytic oxidation (40 turnovers) of dimethyl sulfoxide to the sulfone with >90% current efficiency. The tetrabutylammonium salt of **1** in acetonitrile solution catalyzes the epoxidation of *trans*-stilbene by iodosylbenzene. Reduction of **2** to a heteropoly blue is not possible, due to catalytic hydrogen evolution, except in the presence of dimethyl sulfoxide which is catalytically reduced (30 turnovers) to dimethyl sulfide with ca. 50% current efficiency. Preliminary experiments show that the behavior of $\alpha_2$-$[P_2W_{17}O_{61}Ru^{III}(H_2O)]^{7-}$ parallels that of **1**.

## Introduction

The possibility of incorporating transition-metal cations into "octahedral" binding sites on the surfaces of lacunary heteropolyanions such as $[SiW_{11}O_{39}]^{8-}$ and $[P_2W_{17}O_{61}]^{10-}$ (Figure 1) results in the formation of complexes, $[SiW_{11}O_{39}M(L)]^{n-}$ etc., that bear many similarities to metal complexes of macrocyclic ligands, e.g. the metalloporphyrins and related species. This has excited considerable recent interest and activity, for it has been pointed out that the robust nature of the oxometalate "ligands" and their resistance to oxidation lead to valuable potential applications in catalysis, especially since it is possible to work with these species in both polar and nonpolar solvents.[1-5]

**Table I.** Reduction Potentials of $[PW_{11}O_{39}Ru(L)]^{4-/5-}$ and $^{31}P$ Chemical Shifts of $[PW_{11}O_{39}Ru^{II}(L)]^{5-}$

| L | $E(Ru^{III/II})$, V vs SCE | $^{31}P$, ppm | $\nu_{1/2}$, Hz |
|---|---|---|---|
| $Me_2SO$ | +0.33 | −10.8 | 2.0 |
| $(CH_2)_4SO$ | +0.33 | −10.8 | 2.4 |
| $Ph_2SO$ | +0.38 | −10.7 | 2.5 |
| $Me_2S$ | +0.11 | −10.8 | 32 |
| Me-cysteine | +0.17 | −10.7 | 3.2 |
| maleic acid | +0.63 | −10.6 | 2.0 |
| fumaric acid | +0.63 | −10.1 | 1.5 |
| crotonic acid | +0.48 | −10.5 | 2.1 |
| 1,4-dihydroxybut-2-ene | +0.41 | −10.6 | 2.5 |
| pyridine | +0.03 | −75[a] | 1300[a] |

[a] Paramagnetic Ru(III) derivative.

When viewed as ligands, heteropolyoxometalates[6] exhibit an unusual combination of properties. The lacunary anions present

---

[1] (a) Katsoulis, D. E.; Pope, M. T. *J. Am. Chem. Soc.* **1984**, *106*, 2737. (b) Katsoulis, D. E.; Pope, M. T. *J. Chem. Soc., Chem. Commun.* **1986**, 1186. (c) Harmalker, S. P.; Pope, M. T. *J. Inorg. Biochem.* **1986**, *28*, 85. (d) Katsoulis, D. E.; Tausch, V. S.; Pope, M. T. *Inorg. Chem.* **1987**, *26*, 215. (e) Piepgrass, K.; Pope, M. T. *J. Am. Chem. Soc.* **1989**, *111*, 753. (f) Katsoulis, D. E.; Pope, M. T. *J. Chem. Soc., Dalton Trans.* **1989**, 1483.

0002-7863/92/1514-2932$03.00/0